Published in final edited form as:
Biochemistry. 2008 July 22; 47(29): 7663–7672. doi:10.1021/bi800545n.

Arginine Coordination in Enzymatic Phosphoryl Transfer: Evaluation of the Effect of Arg166 Mutations in *Escherichia coli* Alkaline Phosphatase[†,‡]

Patrick J. O'Brien[§,⊥], **Jonathan Kyle Lassila**[§], **Timothy D. Fenn**[‖], **Jesse G. Zalatan**[#], and **Daniel Herschlag**[*,§]

§ *Department of Biochemistry, Stanford University, Stanford, California 94305*

‖ *Department of Molecular and Cellular Physiology, Stanford University, Stanford, California 94305*

 # Department of Chemistry, Stanford University, Stanford, California 94305

Abstract

Arginine residues are commonly found in the active sites of enzymes catalyzing phosphoryl transfer reactions. Numerous site-directed mutagenesis experiments establish the importance of these residues for efficient catalysis, but their role in catalysis is not clear. To examine the role of arginine residues in the phosphoryl transfer reaction, we have measured the consequences of mutations to arginine 166 in *Escherichia coli* alkaline phosphatase on hydrolysis of ethyl phosphate, on individual reaction steps in the hydrolysis of the covalent enzyme-phosphoryl intermediate, and on thio-substitution effects. The results show that the role of the arginine side chain extends beyond its positive charge, as the Arg166Lys mutant is as compromised in activity as Arg166Ser. Through measurement of individual reaction steps, we construct a free-energy profile for the hydrolysis of the enzyme-phosphate intermediate. This analysis indicates that the arginine side chain strengthens binding by ~3 kcal/mol and provides an additional 1-2 kcal/mol stabilization of the chemical transition state. A 2.1 Å x-ray diffraction structure of Arg166Ser AP is presented, which shows little difference in enzyme structure compared to the wild-type enzyme, but shows a significant reorientation of the bound phosphate. Altogether, these results support a model in which the arginine contributes to catalysis through binding interactions and through additional transition state stabilization that may arise from complementarity of the guanidinum group to the geometry of the trigonal bipyramidal transition state.

Phosphoryl transfer reactions are fundamental to life. Phosphorylation and dephosphorylation events drive metabolic pathways and cell signaling, while organophosphate compounds allow preservation of genetic information and the transfer of cellular energy (1). Although the enzymes that catalyze phosphoryl transfer reactions are diverse and employ a variety of

[†]This work was supported by a grant from the NIH to D.H. (GM64798). J.K.L. was supported by an NIH postdoctoral fellowship (F32 GM080865). T.D.F. was supported by the Universitywide AIDS Research Program of the University of California (F03-ST-216). J.G.Z. was supported by a Hertz Foundation Graduate Fellowship. Facilities used for x-ray crystallography in the laboratory of Axel T. Brunger were supported by Howard Hughes Medical Institute. The Stanford Synchotron Radiation Laboratory (SSRL) Structural Molecular Biology Program is supported by the Department of Energy, Office of Biological and Environmental Research, and by the NIH, National Center for Research Resources, Biomedical Technology Program, and the National Institute of General Medical Sciences.

[‡]Coordinates and structure factors have been deposited in the RCSB Protein Data Bank as entry 3CMR.

[*]Address correspondence to D.H. at the Department of Biochemistry, Beckman Center, B400, Stanford University, Stanford, CA 94305-5307. Phone 650-723-9442. Fax: 650-723-6783. Email: herschla@stanford.edu

[⊥]Current Address: Department of Biological Chemistry, University of Michigan

different cofactors (2-5), many contain active site arginine residues that make contacts to the transferred phosphoryl group.

In many enzymes, including creatine kinase, adenylate kinase, F1-ATPase, acetate kinase, protein tyrosine phosphatases, and certain GTPase activating proteins (GAPs), the interactions of these active site arginines are not replaceable by lysine, suggesting that the simple presence of positive charge does not fully describe the arginine contribution (6-11). The guanidinium group itself may be especially suited to binding phosphate because of its ability to form two simultaneous hydrogen-bonding interactions with phosphate oxygens (12-15). However, mutagenesis studies in several enzymes have found that loss of the arginine side chain yields dramatic reduction in catalysis without apparent changes in substrate affinity, raising the possibility of specificity of the arginine interactions for transition state charge and/or geometry (8-11,16).

It is not obvious how these arginine interactions stabilize transition states. Arginine 166 of *Escherichia coli* alkaline phosphatase (AP) is a prime example. Based on crystal structures with various ligands including a vanadyl transition state analog, Arg166 is expected to make two contacts to the nonbridging oxygens in the phosphoryl transfer transition state, while two Zn^{2+} ions provide a template for the nucleophile, leaving group oxygen, and the other non-bridging phosphoryl oxygen (17-19) (Figure 1).

To address the question of how Arg166 could provide stabilization in the transition state, it is important to consider what might happen to negative charge on the nonbridging oxygens during the progression to the transition state. Isotope effect and linear free energy relationship studies point to a loose transition state for transfer of a phosphoryl group from a phosphate monoester in solution (20-23). In this loose transition state, bond breakage with the leaving group has progressed further than bond formation to the nucleophile, so that there is a net *loss* of electrons from the phosphoryl group (23,24). There is no reason to expect that a net loss of electrons experienced by the phosphoryl group would lead to an increase in negative charge on its nonbridging oxygens (24,25). Computational studies of metaphosphate suggest that the charge on these oxygens may not change significantly during progression to the metaphosphate-like loose transition state (26-28). Thus, it is not obvious how interaction with positively charged arginine side chains would stabilize this transition state.

In part because of this paradox, a prevalent idea in the literature has been that the positively charged residues seen in numerous active sites result in a tighter transition state with increased negative charge on the nonbridging oxygens and favorable interactions with the positively charged side chains (see examples cited in reference 29). However, isotope effect and linear free energy relationship studies have shown no evidence that the transition states for phosphoryl transfer differ between the AP-catalyzed and the uncatalyzed reactions (29-35). Furthermore, no apparent change in transition state character was found when either the positively charged Arg166 was removed by mutagenesis (29) or when substrates with less nonbridging oxygen negative charge were tested (36). Thus, the available experimental evidence suggests that the AP-catalyzed reaction proceeds through a loose transition state similar to that in solution, and the question remains—how do positively charged arginine side chains contribute to catalysis if there is not an expectation of developing negative charge on the nonbridging oxygens?

Studies with protein tyrosine phosphatases (PTPases) led to a model in which the rigid geometry of the arginine guanidinium group was crucial for achieving ideal hydrogen-bonding interactions in the transition state that in turn serve to position the molecule for optimal transition state stabilization by other active site elements (8,37-39). To evaluate and possibly extend this model, it is desirable to obtain structural information about the effects of the arginine residue and to quantify the effect of the arginine-phosphoryl interaction on both substrate

binding and the rate of the chemical transformation. Because k_{cat} and K_M values do not necessarily provide this information directly (40), we have measured the effect of arginine mutations on the rates and equilibrium constants for individual reaction steps in alkaline phosphatase. To further assess the role of the arginine, we have compared the x-ray structure of AP with and without this active site arginine and we have studied the effect of mutations in this residue on reactivity with various substrates, including phosphorothioates, where sulfur replaces one of the nonbridging phosphoryl oxygens.

Alkaline phosphatase provides a good system for testing the proposed model for several reasons. Much work over the past decades has provided a good model for the transition state and its interactions in the AP active site (17-19,29-36). The enzyme's reaction cycle has been established, and individual reaction steps can be monitored to determine the effect of arginine mutations on binding and catalysis (18,41). Mechanistic studies (29) and an x-ray diffraction structure presented herein provide a context for interpreting the effects of arginine mutation in AP. Finally, AP and the PTPases have similar phosphoryl group-arginine contacts, but their remaining active site interactions are very different, with the PTPases employing primarily backbone amide contacts to the phosphoryl group rather than the metal ions used by AP (42).

The results presented here indicate that arginine strengthens binding of inorganic phosphate (P_i), stabilizes the transition state for phosphoryl transfer, and helps to position the substrate for reaction. These results complement numerous prior observations of arginine-phosphoryl interactions important for catalysis (6-11,16). Analysis of the results presented here and prior work is consistent with a physical model in which there is a geometrical preference for interaction of arginine with two equatorial oxygen atoms in the trigonal bipyramidal transition state for phosphoryl transfer (37-39).

MATERIAL AND METHODS

Materials

p-Nitrophenyl phosphate (pNPP) was obtained from Sigma. ^{32}P-labeled ethyl phosphate (EtOP) was synthesized from ^{32}P-γ-labeled ATP and ethanol as previously described (33). *p*-Nitrophenyl *O*-phosphorothioate (pNPPS) was synthesized previously (31).

Purification of Alkaline Phosphatase

Plasmids for expression of AP and Arg166Ser AP were provided by E.R. Kantrowitz (43). The plasmid for expression of Arg166Lys AP was provided by D. Kendall (44). Wild-type and mutant forms of AP were purified as previously described (45). Protein concentrations were determined from the absorbance using $\varepsilon_{278} = 6.7 \times 10^4\ M^{-1}\ cm^{-1}$ for a dimer of molecular weight 94 kD (46).

Steady state spectroscopic assays

Hydrolysis of pNPP was followed by a continuous assay, monitoring the increase in absorbance at 410 nm due to *p*-nitrophenolate formation ($\varepsilon_{410} = 1.62 \times 10^4\ M^{-1}cm^{-1}$ at pH 8). Unless otherwise indicated, the standard reaction conditions were 0.1 M MOPS pH 8.0, 0.5 M NaCl, 1 mM $MgCl_2$, and 100 μM $ZnSO_4$, at 25 °C. By following the full course of the reaction it was possible to obtain excellent data with as little as 0.1 μM substrate. Use of such low substrate concentrations is critical because of the very strong inhibition by the inorganic phosphate product (33,47,48). Inhibition constants (K_i) for inorganic phosphate were measured as previously described (33). Hydrolysis of pNPPS was measured with the same procedure and under the same conditions.

^{32}P-based assay for determination of k_{cat}/K_M with alkyl phosphate substrates

Reactions of alkyl phosphates were carried out as previously described using the standard reaction conditions described above and ^{32}P-labeled substrates (33). Reactions were followed to completion (≥5 half-lives), and the rate constants were obtained by nonlinear least-squares fit to a single exponential. Reactions were first order in substrate and enzyme in all cases, and this reaction order was confirmed by varying the concentration of both enzyme and substrate over at least a 10-fold range.

^{32}P-based assay for the detection of the covalent E-P intermediate

To measure formation of the covalent intermediate, samples of wild-type or Arg166Ser AP were incubated with ^{32}P-inorganic phosphate (~1 μCi; 6000 Ci/mmol, Amersham Biosciences). In all cases, the desired concentration of inorganic phosphate was obtained by adding unlabeled inorganic phosphate in large molar excess. To improve the efficiency of acid quench, we performed the following experiments at 0 °C. Standard conditions for these experiments were 0.1 M MOPS pH 7.0, 0.5 M NaCl, 1 mM $MgCl_2$, 0.1 mM $ZnSO_4$. The covalent intermediate (E-P) was trapped by rapidly denaturing the sample (50 μL) and precipitating the enzyme by the rapid addition of ice-cold 6 M perchloric acid (500 μL) followed by centrifugation at 18,000 × g for 10 min. The resulting pellet was washed twice with cold 5% trichloroacetic acid (500 μL each) and solubilized with 50 μL SDS-PAGE sample buffer (100 mM Tris•Cl pH 6.8, 50 mM EDTA, 10 mM P_i, 100 mM DTT, 2% SDS, 10% glycerol, and 0.02% Bromophenol Blue). Samples were separated on a 10% SDS-PAGE gel, and the gels were dried and exposed to Phosphorimager cassettes. Typically reactions were performed in duplicate or triplicate and the average value was calculated. A standard curve of radioactivity was generated by spotting known amounts of ^{32}P-inorganic phosphate (analyzed in parallel by liquid scintillation counting) to filter paper and exposing to the same Phosphorimager cassette. By comparison to the standard curve, the amount of radioactivity in the protein band could be readily quantified. Control experiments in which the protein band was visualized with Coomassie Blue and the intensities quantified using Quantity One software (Invitrogen) confirmed that samples of AP (400-4000 ng) were quantitatively precipitated and recovered by this protocol (data not shown).

The equilibrium constant [E•P]/[E-P] (K_3, Scheme 1) was determined by increasing the concentration of inorganic phosphate to the point at which a constant ratio of covalently labeled enzyme to total enzyme ($[E\text{-}P]/[E]_{total}$) was observed, such that essentially all enzyme bound phosphate and $[E]_{total} = [E\text{-}P] + [E\bullet P]$. We found that two hours was sufficient in all cases to reach equilibrium, and control reactions that were incubated for up to 24 hours gave the same result within error. The Arg166Ser mutant required ~500-fold higher concentration of inorganic phosphate to reach saturation, and fits to the dependence of bound phosphate concentration on total phosphate concentration were in excellent agreement with the independently determined K_i value for inorganic phosphate measured under the same conditions (data not shown).

To measure the dephosphorylation rate constant (k_3, Scheme 1), the covalent E-P phosphoenzyme was formed at pH 5.0 and rapidly diluted to the standard reaction conditions that also contained excess unlabeled P_i. To follow the reaction, the E-P phosphoenzyme was quantitated with the aforementioned method at varying time intervals between dilution and acid quench. A pH meter was used to confirm pH values of mock reactions. Because the E•P complex is strongly favored over covalent E-P in the standard reaction conditions, the rate of the reverse reaction is negligible in this experiment and the observed rate constant for dephosphorylation equals k_3.

In addition to the dephosphorylation rate constant, we also evaluated the phosphorylation rate constant by initiating the reaction by adding ^{32}P-labeled P_i to unphosphorylated enzyme and following the formation of E-P as a function of time by acid precipitation and SDS-PAGE analysis, as described above. Because in this case the reverse reaction is significant, the observed rate constant for phosphorylation represents an approach to equilibrium and corresponds to the sum of the forward and reverse rate constants ($k_{obsd} = k_3 + k_{-3}$) (40). The observed rate constant for phosphorylation was the same within error as k_3, confirming that the equilibrium is strongly in favor of E•P. Values of k_{-3} were calculated from the measured values of k_3 and K_3 ($k_{-3} = k_3/K_3$).

Construction of a free energy reaction profile

To illustrate the kinetic and thermodynamic effects of the Arg166Ser mutation on the reactions of covalent and noncovalent phosphate species, a free energy reaction profile was calculated for a standard state of 0 °C, pH 7.0, 1 nM enzyme, and 10 mM inorganic phosphate. Phosphate is a true substrate of AP, because the enzyme catalyzes the exchange of ^{18}O from water into P_i (49-53). One can therefore envision a symmetrical free energy profile in which $1/K_1 = K_4$ and $1/K_2 = K_3$ (Scheme 1, with R = H). At pH 7 and higher, negligible covalent phosphoenzyme forms and K_4 is approximated by the inhibition constant for P_i($K_4 \sim K_i$). The value of K_3 was determined as described above. These equilibrium constants were converted to ΔG values with the equation: ΔG = -RTlnK, in which K is the equilibrium constant corrected to the standard state, R is the gas constant (0.001987 kcal/K•mol) and T is 273 K. To determine the height of the barrier between each species, we used the equation: $\Delta G^{\ddagger} = -RT\ln(hk/k_BT)$, in which k is the rate constant, h is Planck's constant (1.58×10^{-37} kcal•s) and k_B is the Boltzmann constant (3.3×10^{-27} kcal/K). The microscopic rate constants were determined as described above and listed in Table 4.

Our estimate of k_{-4} (the second order rate constant for binding of P_i, Scheme 1) is based on the observed k_{cat}/K_M value of $\sim 3 \times 10^7$ $M^{-1}s^{-1}$ for the reaction of pNPP, phenyl phosphate, and propargyl phosphate (33) as the binding of these substrates must be at least this fast. With the independently determined value of $K_i = K_4$, the value of k_4 was calculated as $k_4 = k_{-4}K_4$. The resulting values of k_4, k_{-4}, and K_4 for wild-type AP are in good agreement with values obtained in two independent studies, one measuring K_4 of 2.3×10^{-6} M by comparison of transphosphorylation and hydrolysis reactions (54) and the other measuring k_4 of 30 s^{-1} by ^{31}P NMR inversion transfer experiments (55).

Crystallization and Structure Determination

For crystallization, a slightly different protein preparation of the Arg166Ser mutant was used, based on the pMAL-p2X maltose-binding fusion construct (New England Biolabs) (Ref. 67 and J.G.Z, T.D.F., D.H., manuscript in preparation). This preparation yields the full-length protein, residues 1-449, while constructs using the native periplasmic export tag yield residues 1-449 plus an extra N-terminal arginine arising from the signal peptide. Enzyme purified by this method and by the previously discussed method (45) yielded identical rate constants (data not shown).

The Arg166Ser mutant of AP crystallized in space group $P6_322$ with one dimer per asymmetric unit from a mother liquor solution of 22% PEG 3350, 0.2 M sodium citrate, pH 5.8, 1mM $MgCl_2$, and 5 mM $NaHPO_4$. Hanging drop trays were incubated at 20°C and the protein solution was at 7 mg/mL. Crystals were cryo-protected with 30% glycerol in mother liquor and data were collected at the Stanford Synchotron Radiation Laboratory (SSRL).

Data were processed with DENZO and SCALEPACK (56). Five percent of reflections were set aside for calculation of R_{free}. Molecular replacement phasing was performed with Phaser

(57) using wild-type AP (pdb 1ALK) as a search model. Phenix (58) was used for initial refinement, with each run followed by visual inspection and adjustment with Coot (59**)**. σ_A-weighted $2F_o$-F_c and F_o-F_c maps were inspected at each step and used to guide model building. After initial refinement with Phenix, the Arg166Ser structure was further refined with Refmac, including a final stage with TLS refinement of each monomer (60).

RESULTS AND DISCUSSION

The experiments presented herein probe the role of the active site arginine residue of AP. We present new results and summarize previous results for the effect of mutation of this residue on overall catalysis, on individual reaction steps, and on the magnitude of the thio-effect – *i.e.*, the rate effect upon substitution of a nonbridging phosphoryl oxygen atom with sulfur.

Overall effect of Arg166 mutations

Prior studies reported that mutation of Arg166 to Ala reduced k_{cat}/K_M for *p*-nitrophenyl phosphate (pNPP) ~3-300-fold, depending on conditions (32,43). The range of values presumably reflects, at least in part, the problem of phosphate product inhibition that arises in assays commonly employed for AP (33,47,48). An effect of 330-fold on k_{cat}/K_M is observed upon mutation of the Arg residue to Ser, when care is taken to avoid phosphate inhibition (45,61). This value should represent a lower limit for the effect of removal of the Arg residue on the overall binding and chemical transformation because binding rather than the chemical step is rate limiting for the reaction of pNPP with the wild-type enzyme (22,62,63).

To evaluate the effect of Arg166 mutations on a substrate for which the chemical step is rate limiting, we compared the reactions of ethyl phosphate for the wild-type and mutant enzymes (Table 1). The observed deleterious effect of 5800-fold is 18-fold larger than that obtained with pNPP (Table 1). Importantly, the same deleterious effect, within two-fold, is observed when Arg166 is replaced with Lys instead of Ser. Thus, the role of Arg extends beyond merely supplying a positive charge in the active site.

Effect of Arg166 mutations on phosphate inhibition

To investigate the effect of Arg166 mutations on binding we turned to inhibition by inorganic phosphate (P_i). This strategy was necessary because values of K_M for AP substrates do not, in general, represent equilibrium dissociation constants. Instead, there is a change in rate-limiting step during the progression from subsaturating conditions to saturating conditions. Under subsaturating conditions, binding or formation of the covalent E-P phosphoenzyme (k_1 or k_2, Scheme 1) is rate limiting, depending on the substrate (22,62,63). Under saturating conditions, rates are limited by hydrolysis of the E-P phosphoenzyme (k_3) at low pH and by release of bound P_i (k_4) at high pH (18,48,63,64).

We therefore assessed effects on binding of P_i using inhibition experiments. At the pH used for these experiments, pH 8, the noncovalent E•P_i complex accumulates so that the observed inhibition constant is equal to the dissociation constant for P_i ($K_i^{Pi} = K_d^{Pi} = K_4$) (49). Experiments and analyses below show that this relationship holds for the mutant enzymes as well. Mutation of the active site Arg to Ser decreases binding by 420-fold **(**Table 2**)**; similar effects on K_i^{Pi} were observed for the Arg166Ala mutation (43) and also presumably reflect weakening of the noncovalent complex. A value of K_i^{Pi} measured in a prior study (43) for the Arg166Ser mutant was in good agreement with our value. However, the prior study reported 13-fold higher K_i^{Pi} for the wild-type enzyme, and the earlier, higher value may be due to the effect of inorganic phosphate liberated as a product of the reaction, which, as noted above, was a common problem in some earlier AP assays (33,47,48). Our value for wild type ($K_i^{Pi} = K_4$

= 1.1×10^{-6} M) is in good agreement with the value of 2.3×10^{-6} M measured by comparison of transphosphorylation and hydrolysis reactions (54).

The Arg166Lys mutant binds P_i 6-fold more strongly than the Ser mutant (Table 2), suggesting that a ground state interaction is made with the positively charged Lys side chain. Despite this favorable ground state interaction, k_{cat}/K_M is not substantially increased for the Lys mutant relative to the Ser mutant, as noted above (Table 1). Thus, even though Lys can interact with and help to stabilize a bound phosphoryl group, it appears that this favorable interaction is not maintained in the transition state for the chemical transformation, underscoring the distinct catalytic properties of Arg.

Structure of Arg166Ser enzyme•phosphate complex at 2.1 Å resolution

To provide a structural context for evaluating further kinetic effects of the Arg166Ser mutation, we have determined an x-ray crystallographic structure of this mutant enzyme with noncovalently bound phosphate (Table 3). The structure shows no significant overall change relative to wild-type AP. Mutant and wild-type (pdb 1ALK, Ref. 17**)** structures overlay with 0.3 Å RMSD over all alpha carbons in both chains of the dimeric enzymes.

Within the active site, very little difference is observed between the mutant and wild-type enzymes other than the obvious side chain mutation. The positions of Asp101 and Asp153, active site groups that interact with Arg166 in the wild-type enzyme, remain unchanged in the mutant enzyme. The positions of the Zn^{2+} ions and their six ligands are very similar to those in wild-type AP structures (Figure 2A,B). Zn^{2+}-Zn^{2+} distances differ on average by less than 0.1 Å with unliganded wild-type structure 1ED9 (65) and by 0.3 Å with phosphate-bound wild-type structure 1ALK. While the Mg^{2+}-ligand distances are slightly longer than those in the 1ALK structure, with a mean distance of 2.2 Å in the mutant structure and 2.0 Å in 1ALK, the differences are small and highly subject to conditions including the resolution and refinement procedures used in structure determination. Thus, while the static structural information provided by x-ray diffraction data do not allow us to fully rule out subtle changes that might occur as a result of mutation, the 2.1 Å structure of the Arg166Ser mutant shows no evidence that the mutation causes any unexpected, chemically significant change in the active site of the enzyme.

The major difference between the Arg166Ser and wild-type structures is in the position of noncovalently bound phosphate (Figure 2C). In the wild-type structure, phosphate is oriented to form hydrogen bonds with Arg166 (distances 2.64 Å and 2.61 Å in 1ALK chain A). The position of noncovalently bound inorganic phosphate in the wild-type structure is confirmed by the 1ED8 wild-type structure (65**)**. However, the Arg166Ser mutant structure shows the phosphate rotated and translated away from the Ser102 nucleophile and out of alignment with the position of the guanidinium group in the wild-type enzyme (Figure 2C). When compared to the wild-type structure in complex with transition state analog vanadate (1B8J, Ref. 19**)**, the phosphate in the wild-type enzyme is clearly aligned with the transition state analog, while the phosphate in the mutant enzyme is rotated and translated such that the phosphorous and vanadate atoms differ in position by 1.3 Å in aligned structures (Figure 2C). The oxygen atoms are shifted by 0.6-3.1 Å relative to phosphate oxygens in the wild-type structure.

Relative to the mutant structure, it appears that in the wild-type enzyme, the interaction with Arg166 results in an orientation of bound phosphate that is closer to the nucleophile and appears to bring the phosphate closer to a transition-state-like alignment with the Zn^{2+} ions. This observed repositioning of the phosphate in the presence of Arg166 is consistent with a favorable ground-state binding interaction between the phosphate and guanidinium groups. To quantify the energetic contribution of this interaction with Arg166 for binding and the catalytic step, we have measured individual equilibria and reaction rates in the wild-type and mutant enzymes.

Effects on equilibria and individual rates in the covalent E-P phosphoenzyme

The overall effect of the Arg166Ser mutation of 5800-fold on k_{cat}/K_M for ethyl phosphate is ~14-fold larger than that on binding of inorganic phosphate (Tables 1 and 2**)**, suggesting that Arg provides specific enhancement in the chemical step. However, this comparison is between binding of phosphate and catalysis of ethyl phosphate hydrolysis, and it would be preferable to assess relative effects on binding and catalysis more directly.

We cannot directly measure the reaction of phosphate esters bound to AP in a Michaelis complex (k_2, Scheme 1) because this step is not rate-limiting under steady-state conditions for most substrates, because inhibition from contaminating P_i complicates steady-state kinetic analysis of reactions of other substrates, and because weak binding and fast reactions of substrates prevents utilization of standard pre-steady-state approaches to determine the rate of the chemical step (22,48,62-64). We therefore monitored the reaction of the covalent enzyme-phosphate intermediate (E-P). As discussed in Materials and Methods, P_i is itself a substrate of AP, as the enzyme catalyzes the exchange of ^{18}O from water into P_i (49-53).

The rate constants and equilibrium constant for formation and breakdown of the covalent E-P phosphoenzyme were determined as described in Materials and Methods and are compared for wild-type and Arg166Ser AP in Table 4. The value obtained for wild-type K_3 was in good agreement with that measured in an earlier study through comparison of hydrolysis and transphosphorylation reactions (54). There is a small effect of about twofold on the overall equilibrium constant for formation of the E-P phosphoenzyme upon removal of the active site Arg, whereas the rate of formation and breakdown of this adduct are both reduced by about an order of magnitude. Evidence suggests that Arg166Lys AP, which maintains the side chain positive charge, is affected similarly to the Arg166Ser mutant, again underscoring the inability of Lys to replace Arg in the AP active site. [1]

Combining the binding and reactivity data reveals that the active site Arg residue provides similar binding energy, and presumably similar binding interactions, with noncovalently and covalently bound phosphate, but that these interactions strengthen in the chemical transition state. Figure 3 shows free energy profiles for the wild-type and Arg166Ser reactions. The active site Arg residue contributes 1-2 kcal/mol of preferential binding energy for the reaction's transition state relative to the preceding and following ground states, E-P and E•P_i. The observation that Arg stabilizes the transition state relative to both the covalently bound (E-P) and the noncovalently bound (E•P) species suggests specificity of Arg interactions for the transition state relative to species with different orientations and constraints. The energetics and role of these interactions is discussed further below (see *Role of Arginine in Phosphoryl Transfer*).

Effects of thio-substitution on Arg166 mutants

As substitution of a nonbridging oxygen atom of the transferred phosphoryl group with sulfur substantially lessens the deleterious effect of the Arg166 to Ala mutation (32**)**, we further investigated the interplay between thio-effects and this residue **(**Table 5). The substitution of

[1]The comparison of rate constants for hydrolysis of E-P for the Arg166Ser and Arg166Lys mutants is based on the similar observed values of k_{cat} for reaction of pNPP for these mutant enzymes (Table 1**)**. Our assumption that k_{cat} for Arg166Lys AP with pNPP as a substrate is dominated by hydrolysis of the covalent intermediate ($k_{cat} = k_3$) is supported by a previous study carried out by Butler-Ransohoff and colleagues, in which Arg166Lys AP and saturating concentration of pNPP were mixed in a stopped-flow spectrophotometer **(**44**)**. A rapid pre-steady state burst of *p*-nitrophenolate release was observed that was followed by a slower steady state rate. This result indicates that steady state hydrolysis of pNPP is limited either by hydrolysis of the E-P intermediate (k_3) or phosphate release (k_4, Scheme 1). The relative weak affinity for P_i that we observed suggests that k_3 is the rate-limiting step rather than dissociation of P_i. Indeed, k_4 is predicted to be at least an order of magnitude greater than the value of $k_{cat} = 0.65\ s^{-1}$, as k_{cat}/K_M with pNPP as a substrate reflects a lower limit for binding of a phosphate ester ($k_{-4} \geq 1.9 \times 10^5\ M^{-1}\ s^{-1}$) such that: $k_4 \geq k_{-4} \times K_d = (1.9 \times 10^5\ M^{-1}\ s^{-1}) \times (75 \times 10^{-6}\ M) = 14\ s^{-1}$].

sulfur for oxygen results in an increase in bond length of about 0.5 Å, an increase in van der Waals radius of about 0.3 Å, an increase in mean hydrogen bond lengths of about 0.5 Å and a decrease in mean equilibrium hydrogen bonding angles of about 20° (66). These effects would be expected to substantially alter a precise Arg-phosphoryl geometry that is enforced through dual hydrogen bonds of the rigid guanidino group (Figure 1). This model is supported by the large 6000-fold thio-effect (ratio of phosphate to phosphorothioate activities) seen in the wild-type enzyme (Table 5).

The large thio-effect on reaction of pNPP with the wild-type enzyme is reduced by 160-fold upon mutation of the Arg residue to Ser, because the loss of the arginine side chain has a large effect on the phosphate reaction but very little effect on the phosphorothioate reaction. The remaining thio-effect in Arg166Ser has been suggested to arise because of a redistribution of charge in the transferred phosphoryl group upon thio-substitution that leaves less charge on the phosphoryl oxygen atom situated between the two active site Zn^{2+} ions and thus a reduced electrostatic interaction energy with the Zn^{2+} ions **(**67).

A significant loss of thio-effect upon mutation of Arg is the predicted effect of a model in which the geometry of the arginine-phosphoryl interaction is crucial for its function in catalysis (37). Thus, when the Arg is present, disruption of the interaction by sulfur substitution results in a large effect, but in the absence of the Arg, there is no beneficial interaction to disrupt by sulfur substitution. Indeed, the thio-effects in Arg166Lys, Arg166Ser, and Arg166Ala are all reduced substantially relative to wild type, suggesting generality of this effect, even in the presence of positively charged lysine (Table 5).

The Lys mutant shows only a small thio-effect (12-fold) and, surprisingly, it hydrolyzes the thio-substrate 3-fold faster than wild-type AP (Table 5). Thus, Lys can interact preferentially with the transferred thiophosphoryl group in the reaction's transition state, relative to an Arg residue. The preferential catalysis with Lys is likely due to a favorable interaction of the positively charged amine side chain with the transferred thiophosphoryl group; the mutant with Ser in position 166 gives a reaction rate almost an order of magnitude slower than that for the Lys mutant (Table 5). We speculate that lysine offers an advantage over arginine in contacting the thiophosphoryl transition state because its size and flexibility allow it to maintain contact, while the larger, more rigid Arg guanidino group faces greater displacement and disruption from the thio-substitution.

Role of arginine in phosphoryl transfer

A possible role for arginine coordination in phosphoryl transfer was described in prior work on protein-tyrosine phosphatases, which have a very similar dual hydrogen-bonding interaction between arginine and the transferred phosphoryl group (8,37-39). In this model, the geometrically rigid contact of the guanidinium group enforces optimal hydrogen-bonding geometry in the transition state of the reaction, when the nonbridging oxygen atoms are arranged in trigonal bipyramidal configuration with the leaving group and nucleophile oxygens. Thus, the hydrogen bonds would increase in strength during progression from tetrahedral substrate to trigonal bipyramidal transition state, and the guanidinium group would specify positioning and geometry of the phosphoryl group that allows optimal electrostatic stabilization by the Zn^{2+} ions and other active site elements. An increase in hydrogen bond strength during progression to the transition state could be caused by a variety of effects, including a shortening of the hydrogen bonds due to change in orientation and geometry of the phosphoryl group in the transition state (37,39**)** or through a tightening of the number of rotational and translational states accessible to the phosphoryl group in progression to the transition state. Either possibility is consistent with favorable transition state interactions due to the relative rigidity of the guanidinium group when engaged in dual contacts to the phosphoryl group. An overlay of the Arg166Ser-phosphate complex structure and structures

of wild type with phosphate and transition state analogue vanadate provide structural support for favorable interactions of the Arg166 guanidinium group with the nonbridging oxygens in a transition-state-like orientation (Figure 2C).

The various measurements from this study allow us to estimate energetic values for the Arg-phosphoryl interaction in the transition state by comparison between wild-type and Arg166Ser AP. Although mutagenesis always leaves open the possibility that unintended consequences contribute to the energetic changes, we expect that comparison of wild-type and Arg166Ser AP allows a reasonable approximation of the contribution of the Arg-phosphoryl interaction. The crystal structure of Arg166Ser AP reported herein shows no evidence of unintended structural changes to the active site as a consequence of mutation. Furthermore, linear free energy relationships indicate no evidence of mechanistic changes in Arg166Ser relative to wild type (29**)**.

Thus, we have estimated the energetic contribution of the Arg-phosphoryl interaction in two ways. First, the comparison of k_{cat}/K_M with EtOP for wild type and Arg166Ser yields a 5.1 kcal/mol difference in stabilization of the transition state between the two enzymes, relative to free enzyme and substrate. Second, as shown in the free energy diagram obtained for the hydrolysis of the E-P phosphoenzyme (Figure 3), relative to free enzyme and phosphate, the wild-type enzyme provides 4.5 kcal/mol more stabilization to the transition state than Arg166Ser. Although both analyses are subject to concern that there may be secondary consequences of mutation, they present a consistent estimate of a 4-5 kcal/mol stabilizing interaction for binding and catalysis, relative to free enzyme and substrate in solution. For comparison, the total transition state stabilization for pNPP hydrolysis by R166S AP relative to the uncatalyzed hydrolysis under standard conditions is 21 kcal/mol (45).

Combined with measurement of individual reaction steps, this 4-5 kcal/mol estimate can be further dissected into bound state and transition state contributions. As shown in Figure 3, the E•P and E-P complexes are stabilized by 3.2 kcal/mol and 2.8 kcal/mol, respectively, in wild type over Arg166Ser. The transition state for hydrolysis of the covalent complex (E-P) is further stabilized by 1.7 kcal/mol in Arg166 compared to Ser166, and the transition state for formation of covalent E-P from the noncovalent complex (E•P) is stabilized by 1.3 kcal/mol in Arg166 in comparison to Ser166. Altogether, these results suggest that the interaction between the Arg166 guanidinium group and the phosphoryl oxygen atoms offers a ~3 kcal/mol ground state interaction and an additional ~1-2 kcal/mol differential stabilization of the transition state.

The results obtained herein for Arg166 of alkaline phosphatase, summarized in Figure 4 along with pertinent prior results, are consistent with the model that Arg residues offer specific stabilization to the phosphoryl transfer transition state through precisely placed contacts. As shown in Figure 4A, lysine provides no significant rate acceleration relative to serine in hydrolysis of ethyl phosphate, indicating that the presence of positive charge is not sufficient to achieve wild-type-like reactivity. At the same time, Lys increases binding of P_i relative to the Ser166 mutant (Figure 4B), suggesting that Lys166 does form an interaction, but that this interaction does not provide specific stabilization in the transition state. The chemical step for hydrolysis of the covalent E-P species (k_3) is enhanced 20-fold by Arg relative to Ser, with a similar effect of Arg relative to Lys (Figure 4C, and see earlier footnote), reflecting the transition state stabilization by Arg. Substitution of a nonbridging phosphoryl oxygen with sulfur is expected to disrupt the geometry of the guanidinium-phosphoryl contact. Thus, the large effect of ~6,000-fold on k_{cat}/K_M in wild-type AP seen upon substitution of a nonbridging oxygen with sulfur (Figure 4D), compared to 6- to 100-fold effects without Arg166, provides further support for a model in which the strength of the Arg interaction is sensitive to its geometry.

Altogether, the results presented here show that the active site arginine of *E. coli* alkaline phosphatase contributes to catalysis both through ground state binding interactions and through specific stabilization of the transition state of the phosphoryl transfer reaction. Analysis of individual reaction steps suggests that the arginine side chain provides ~3 kcal/mol stabilization to the ground state and 1-2 kcal/mol additional stabilization of the phosphoryl transfer transition state. The results support a model in which the guanidinium group engages in hydrogen bonding interactions that attain optimal geometry in the transition state of the reaction. Geometric specificity of arginine interactions for the transition state provides a plausible explanation for the observed transition state specificity, even in the absence of an expectation of increased negative charge on nonbridging oxygens during progression to the transition state. These results help to explain numerous prior studies, which identify large effects upon mutagenesis of arginines in phosphoryl transfer enzymes (6-11,16).

ACKNOWLEDGEMENTS

We thank Dr. Axel T. Brunger for helpful comments on the manuscript and for the use of crystallography facilities. We thank members of the Herschlag lab for helpful comments on the manuscript.

Abbreviations

AP, *Escherichia coli* alkaline phosphatase; pNPP, 4-nitrophenyl phosphate; pNPPS, 4-nitrophenyl phosphorothioate; EtOP, ethyl phosphate; ATP, adenosine triphosphate; MOPS, 3-(N-morpholino)propanesulfonic acid, sodium salt; P_i, inorganic phosphate.

REFERENCES

1. Westheimer FH. Why nature chose phosphates. Science 1987;235:1173–1178. [PubMed: 2434996]
2. Mildvan AS. Mechanisms of signaling and related enzymes. Proteins: Structure, Function, and Genetics 1997;29:401–416.
3. Sträter N, Lipscomb WN, Klabunde T, Krebs B. Two-metal ion catalysis in enzymatic acyl- and phosphoryl-transfer reactions. Agnew. Chem. Int. Ed. Engl 1996;35:2024–2055.
4. Cleland WW, Hengge AC. Enzymatic mechanisms of phosphate and sulfate transfer. Chem. Rev 2006;106:3252–3278. [PubMed: 16895327]
5. Frey, PA.; Hegeman, AD. Enzymatic reaction mechanisms. Oxford University Press; New York: 2006.
6. Gorrell A, Lawrence SH, Ferry JG. Structural and kinetic analyses of arginine residues in the active site of acetate kinase from *Methanosarcina thermophila*. J. Biol. Chem 2005;280:10731–10742. [PubMed: 15647264]
7. Rittinger K, Walker PA, Eccleston JF, Nurmahomed K, Owen D, Laue E, Gamblin SJ, Smerdon SJ. Crystal structure of a small G protein in complex with the GTPase-activating protein rhoGAP. Nature 1997;388:693–697. [PubMed: 9262406]
8. Zhang Z-Y, Wang Y, Wu L, Fauman EB, Stuckey JA, Schubert HL, Saper MA, Dixon JE. The Cys $(X)_5$Arg catalytic motif in phosphoester hydrolysis. Biochemistry 1994;33:15266–15270. [PubMed: 7803389]
9. Jourden MJ, Geiss PR, Thomenius MJ, Horst LA, Barty MM, Brym MJ, Mulligan GB, Almeida RM, Kersteen BA, Myers NR, Snider MJ, Borders CL, Edmiston PL. Transition state stabilization by six arginines clustered in the active site of creatine kinase. Biochimica et Biophysica Acta 2005;1751:178–183. [PubMed: 16005271]
10. Yan HG, Shi ZT, Tsai MD. Mechanism of adenylate kinase. Structural and functional demonstration of arginine-138 as a key catalytic residue that cannot be replaced by lysine. Biochemistry 1990;29:6385–6392. [PubMed: 2119801]
11. Nadanaciva S, Weber J, Wilke-Mounts S, Senior AE. Importance of F_1-ATPase Residue α–Arg-376 for catalytic transition state stabilization. Biochemistry 1999;38:15493–15499. [PubMed: 10569931]

12. Cotton FA, Hazen EE, Day VW, Larsen S, Norman JG, Wong STK, Johnson KH. Biochemical importance of the binding of phosphate by arginyl groups. Model compounds containing methylguanidinium ion. J. Am. Chem. Soc 1973;95:2367–2369.
13. Perreault DM, Cabell LA, Anslyn EV. Using guanidinium groups for the recognition of RNA and as catalysts for the hydrolysis of RNA. Bioorg. Med. Chem 1997;5:1209–1220. [PubMed: 9222514]
14. Hauser SL, Johanson EW, Green HP, Smith PJ. Aryl phosphate complexation by cationic cyclodextrins. An enthalpic advantage for guanidinium over ammonium and unusual enthalpy-entropy compensation. Org. Letters 2000;2:3575–3578.
15. Avenier F, Domingos JB, Van Viliet LD, Hollfelder F. Polyethylene imine derivatives ('Synzymes') accelerate phosphate transfer in the absence of metal. J. Am. Chem. Soc 2007;129:7611–7619. [PubMed: 17530755]
16. Serpersu EH, Shortle D, Mildvan AS. Kinetic and magnetic resonance studies of active-site mutants of staphylococcal nuclease: Factors contributing to catalysis. Biochemistry 1987;26:1289–1300. [PubMed: 3567171]
17. Kim EE, Wyckoff HW. Reaction mechanism of alkaline-phosphatase based on crystal structures: 2-metal ion catalysis. J. Mol. Biol 1991;218:449–464. [PubMed: 2010919]
18. Coleman JE. Structure and mechanism of alkaline phosphatase. Annu. Rev. Biophys. Biomol. Struct 1992;21:441–483. [PubMed: 1525473]
19. Holtz KM, Stec B, Kantrowitz ER. A model of the transition state in the alkaline phosphatase reaction. J. Biol. Chem 1999;274:8351–8354. [PubMed: 10085061]
20. Kirby AJ, Jencks WP. Reactivity of nucleophilic reagents toward pnitrophenyl phosphate dianion. J. Am. Chem. Soc 1965;87:3209–3216.
21. Kirby AJ, Varvoglis AG. Reactivity of phosphate esters: Monoester hydrolysis. J. Am. Chem. Soc 1967;89:415–423.
22. Hengge AC, Edens WA, Elsing H. Transition-state structures for phosphoryl-transfer reactions of p-nitrophenyl phosphate. J. Am. Chem. Soc 1994;116:5045–5049.
23. Hengge AC, Onyido I. Physical organic perspectives on phospho group transfer from phosphates and phosphinates. Curr. Org. Chem 2005;9:61–74.
24. Hengge, AC. Transfer of the Phosphoryl Group. In: Michael, Sinnott, editor. Comprehensive Biological Catalysis: A Mechanistic Reference. 1. Academic Press; San Diego, CA: 1998. Chapter 14
25. Admiraal SJ, Herschlag D. Mapping the transition state for ATP hydrolysis: Implications for enzymatic catalysis. Chemistry & Biology 1995;2:729–739. [PubMed: 9383480]
26. Rajca A, Rice JE, Streitwieser A, Schaefer HF. Metaphosphate and tris(methylene)metaphosphate ($P(CH_2)_3$-) anions: Do they have three double bonds to phosphorous? J. Am. Chem. Soc 1987;109:4189–4192.
27. Horn H, Ahlrichs R. Energetic measure for the ionic character of bonds. J. Am. Chem. Soc 1990;112:2121–2124.
28. Evleth EM, Kassab E, Colonna F, Akacem Y, Ouamerli O. *Ab initio* fitted charges for PO_3^- and related XO_3^n structures. Chemical Physics Letters 1992;199:513–517.
29. O'Brien PJ, Herschlag D. Does the active site arginine change the nature of the transition state for alkaline phosphatase-catalyzed phosphoryl transfer? J. Am. Chem. Soc 1999;121:11022–11023.
30. Weiss PM, Cleland WW. Alkaline phosphatase catalyzes the hydrolysis of glucose-6-phosphate via a dissociative mechanism. J. Am. Chem. Soc 1989;111:1928–1929.
31. Hollfelder F, Herschlag D. The nature of the transition state for enzyme-catalyzed phosphoryl transfer. Hydrolysis of O-aryl phosphorothioates by alkaline phosphatase. Biochemistry 1995;34:12255–12264. [PubMed: 7547968]
32. Holtz KM, Catrina IE, Hengge AC, Kantrowitz ER. Mutation of Arg 166 of alkaline phosphatase alters the thio effect but not the transition state for phosphoryl transfer. Implications for the interpretation of thio effects in reactions of phosphatases. Biochemistry 2000;39:9451–9458. [PubMed: 10924140]
33. O'Brien PJ, Herschlag D. Alkaline phosphatase revisited: Hydrolysis of alkyl phosphates. Biochemistry 2002;41:3207–3225. [PubMed: 11863460]

34. Zalatan JG, Catrina I, Mitchell R, Grzyska PK, O'Brien PJ, Herschlag D, Hengge AC. Kinetic isotope effects for alkaline phosphatase reactions: Implications for the role of active-site metal ions in catalysis. J. Am. Chem. Soc 2007;129:9789–9798. [PubMed: 17630738]
35. Zalatan JG, Herschlag D. Alkaline phosphatase mono- and diesterase reactions: Comparative transition state analysis. J. Am. Chem. Soc 2006;128:1293–1303. [PubMed: 16433548]
36. Nikolic-Hughes I, Rees DC, Herschlag D. Do electrostatic interactions with positively charged active site groups tighten the transition state for enzymatic phoshporyl transfer? J. Am. Chem. Soc 2004;126:11814–11819. [PubMed: 15382915]
37. Zhang Y-L, Hollfelder F, Gordon SJ, Chen L, Keng K-F, Wu L, Herschlag D, Zhang Z-Y. Impaired transition state complementarity in the hydrolysis of O-arylphosphorothioates by protein-tyrosine phosphatases. Biochemistry 1999;38:12111–12123. [PubMed: 10508416]
38. Hoff RH, Wu L, Zhou B, Zhang Z-Y, Hengge AC. Does positive charge at the active sites of phosphatases cause a change in mechanism? The effect of the conserved arginine on the transition state for phosphoryl transfer in the protein tyrosine phosphatase from *Yersinia*. J. Am. Chem. Soc 1999;121:9514–9521.
39. Alhambra C, Wu L, Zhang Z-Y, Gao JL. Walden-inversion-enforced transition state stabilization in a protein tyrosine phosphatase. J. Am. Chem. Soc 1998;120:3858–3866.
40. Fersht, A. Structure and Mechanism in Protein Science. W. H. Freeman and Company; New York: 1999.
41. Reid, TW.; Wilson, IB. *E. coli* alkaline phosphatase. In: Boyer, PD., editor. The Enzymes. Academic Press; New York: 1971. p. 373-415.
42. Zhang Z-Y, Dixon JE. Protein tyrosine phosphatases: Mechanism of catalysis and substrate specificity. Adv. Enzymol. Rel. Areas Mol. Biol 1994;68:1–36.
43. Chaidaroglou A, Brezinski DJ, Middleton SA, Kantrowitz ER. Function of arginine 166 in the active site of *Escherichia coli* alkaline phosphatase. Biochemistry 1988;27:8338–8343. [PubMed: 3072019]
44. Butler-Ransohoff JE, Kendall DA, Kaiser ET. Use of site-directed mutagenesis to elucidate the role of arginine-166 in the catalytic mechanism of alkaline phosphatase. Proc. Natl. Acad. Sci. USA 1988;85:4276–4278. [PubMed: 3288990]
45. O'Brien PJ, Herschlag D. Functional interrelationships in the alkaline phosphatase superfamily: phosphodiesterase activity of *Escherichia coli* alkaline phosphatase. Biochemistry 2001;40:5691–5669. [PubMed: 11341834]
46. Plocke DJ, Levinthal C, Vallee BL. Alkaline phosphatase of *Escherichia coli*: A zinc metalloenzyme. Biochemistry 1962;1:373–378. [PubMed: 14487220]
47. Wilson IB, Snyder SL. Phosphoramidic acids. A new class of nonspecific substrates for alkaline phosphatase from *Escherichia coli*. Biochemistry 1972;11:1616–1623. [PubMed: 4554950]
48. Bloch W, Schlesinger MJ. The phosphate content of *Escherichia coli* alkaline phosphatase and its effect on stopped flow kinetic studies. J. Biol. Chem 1973;248:5794–5805. [PubMed: 4579429]
49. Stein SS, Koshland DE. Mechanism of action of alkaline phosphatase. Arch. Biochem. Biophys 1952;39:229–330. [PubMed: 12997144]
50. Schwartz JH. Phosphorylation of alkaline phosphatase. Proc. Natl. Acad. Sci. USA 1963;49:871–878. [PubMed: 13987375]
51. Applebury ML, Johnson BP, Coleman JE. Phosphate binding to alkaline phosphatase- Metal ion dependence. J. Biol. Chem 1970;245:4968–4976. [PubMed: 4319108]
52. Bock JL, Cohn M. Metal dependence of the phosphate (oxygen)-water exchange reaction of *Escherichia coli* alkaline phosphatase. J. Biol. Chem 1978;253:4082–4085. [PubMed: 350868]
53. Caswell M, Caplow M. Correlation of thermodynamic and kinetic properties of the phosphoryl enzyme formed with alkaline phosphatase. Biochemistry 1980;19:2907–2911. [PubMed: 6994802]
54. Levine D, Reid TW, Wilson IB. The free energy of hydrolysis of the phosphoryl-enzyme intermediate in alkaline phosphatase catalyzed reactions. Biochemistry 1969;8:2374–2380. [PubMed: 4895019]
55. Gettins P, Metzler M, Coleman JE. Alkaline phosphatase: 31P NMR probes of the mechanism. J. Biol. Chem 1985;260:2875–2883. [PubMed: 3882702]

56. Otwinowski Z, Minor W. Processing of X-ray diffraction data collected in oscillation mode. Methods Enzymol 1997;276:307–326.
57. McCoy AJ, Grosse-Kunstleve RW, Storoni LC, Read RJ. Likelihood-enhanced fast translation functions. Acta Cryst 2005;D61:458–464.
58. Adams PD, Grosse-Kunstleve RW, Hung LW, Ioerger TR, McCoy AJ, Moriarty NW, Read RJ, Sacchettini JC, Sauter NK, Terwilliger TC. PHENIX: building new software for automated crystallographic structure determination. Acta Cryst 2002;D58:1948–1954.
59. Emsley P, Cowtan K. Coot: model-building tools for molecular graphics. Acta Cryst 2004;D60:2126–2132.
60. Murshudov GN, Vagin AA, Dodson EJ. Refinement of macromolecular structures by the maximum-likelihood method. Acta Cryst 1997;D53:240–255.
61. O'Brien PJ, Herschlag D. Sulfatase activity of *E. coli* alkaline phosphatase demonstrates a functional link to arylsulfatases, an evolutionarily related enzyme family. J. Am. Chem. Soc 1998;120:12369–12370.
62. Labow BI, Herschlag D, Jencks WP. Catalysis of the hydrolysis of phsophorylated pyridines by alkaline phosphatase has little or no dependence on the pKa of the leaving group. Biochemistry 1993;32:8737–8741. [PubMed: 8395879]
63. Simopoulos TT, Jencks WP. Alkaline phosphatase is an almost perfect enzyme. Biochemistry 1994;33:10375–10380. [PubMed: 8068674]
64. Reid TW, Wilson IB. Conformational isomers of alkaline phosphatase in the mechanism of hydrolysis. Biochemistry 1971;10:380–387. [PubMed: 5543963]
65. Stec B, Holtz KM, Kantrowitz ER. A revised mechanism for the alkaline phosphatase reaction involving three metal ions. J. Mol. Biol 2000;299:1303–1311. [PubMed: 10873454]
66. Platts JA, Howard ST, Bracke BRF. Directionality of hydrogen bonds to sulfur and oxygen. J. Am. Chem. Soc 1996;118:2726–2733.
67. Nikolic-Hughes I, O'Brien PJ, Herschlag D. Alkaline phosphatase is ultrasensitive to charge sequestered between the active site zinc ions. J. Am. Chem. Soc 2005;127:9314–9315. [PubMed: 15984827]
68. Catrina IE, Hengge AC. Comparisons of phosphorothioate and phosphate monoester transfer reactions: Activation parameters, solvent effects, and the effect of metal ions. J. Am. Chem. Soc 1999;121:2156–2163.

Scheme 1.

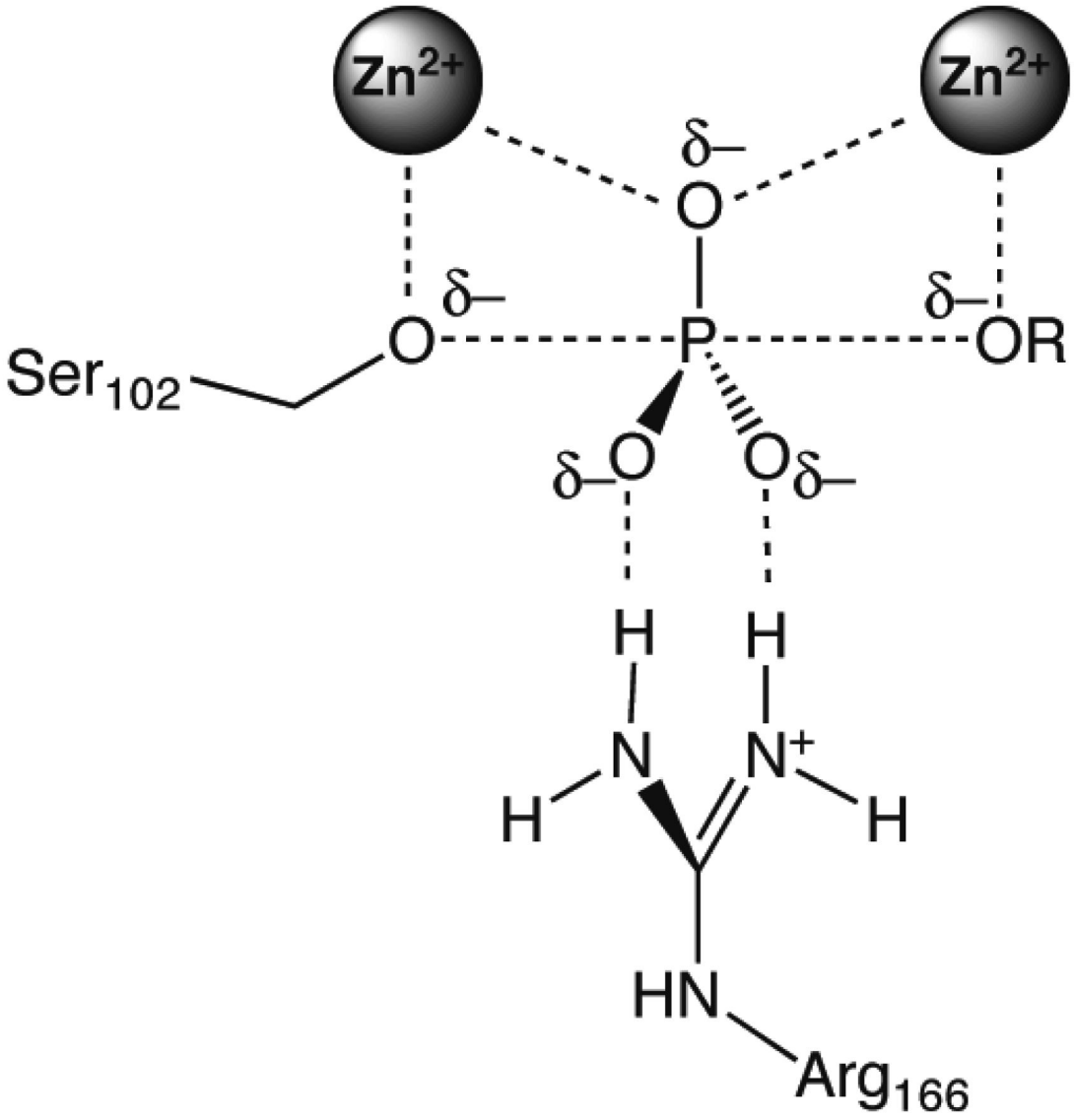

Figure 1.
Expected interactions in the transition state for phosphoryl transfer from a monoester in AP. The oxygen atoms are arranged in trigonal bipyramidal geometry, with one nonbridging oxygen between Zn^{2+} ions, and the others expected to contact Arg166.

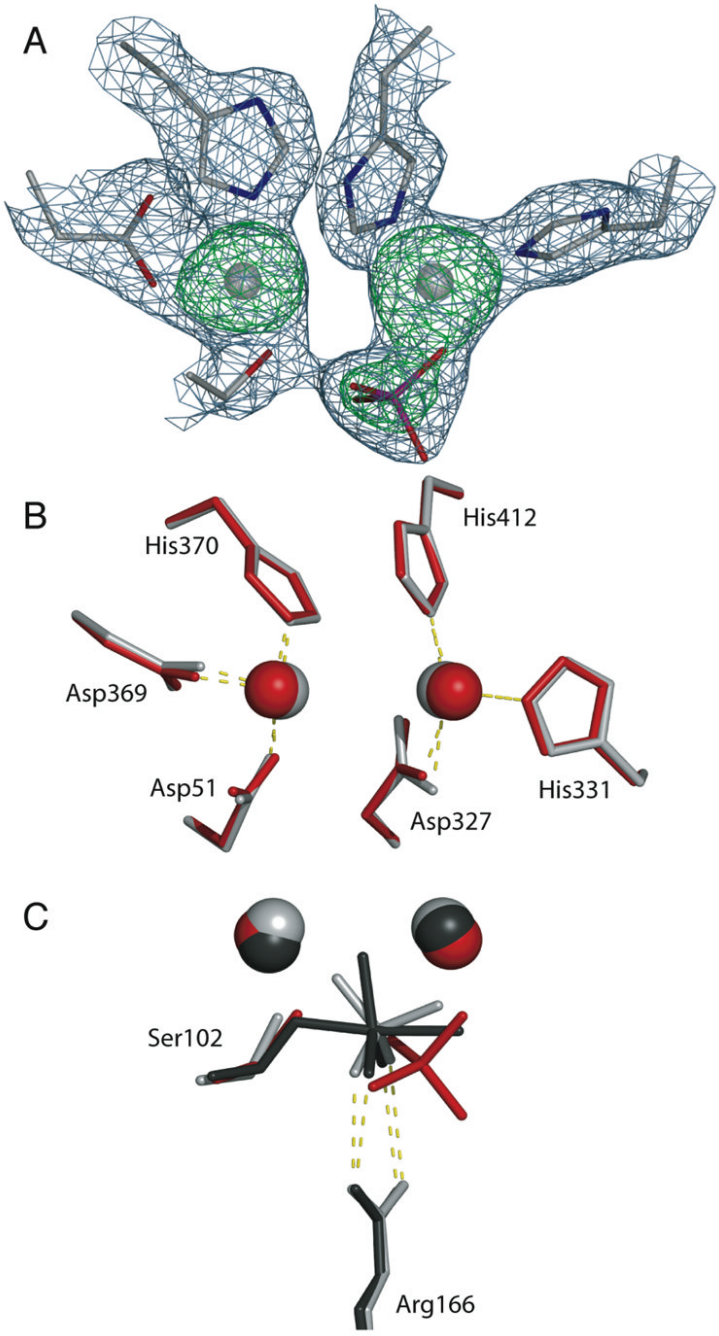

Figure 2.

Arg166Ser active site structure. (A) Simulated annealing omit maps in which the Zn^{2+} ions and phosphate had been omitted from the model. $2F_o$-F_c density is shown in blue and contoured at 1.5 σ. F_o-F_c density is shown in green and contoured at 8 σ. (B) Positions of the two Zn^{2+} ions and six zinc ligands are very similar between the mutant (red) and wild-type (light gray, pdb code 1ED8) structures. (C) The position of bound phosphate is changed significantly in the Arg166Ser enzyme (shown in red) relative to wild type with bound phosphate (light gray, pdb code 1ED8) and wild type with bound transition state analog vanadate (dark gray, pdb code 1B8J). The A chains are aligned by the alpha carbons of the six Zn^{2+} ligands. The distance between phosphorous atoms from mutant and wild-type structures in the aligned structures is

1.3 Å, whereas phosphorous and vanadate atoms in the two wild-type structures are separated by 0.1 Å. In the mutant, the hydroxyl of Ser166 is more than 6 Å away from the nearest phosphate oxygen, and therefore very unlikely to interact with bound phosphate.

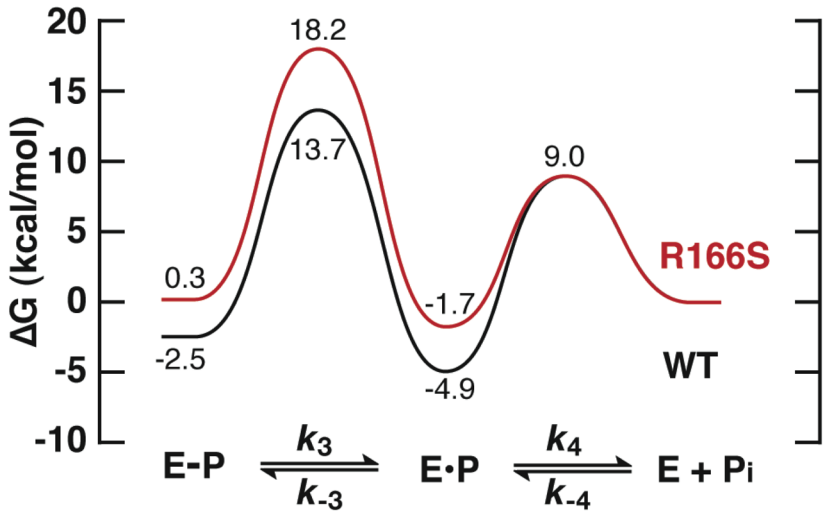

Figure 3.

Free energy profiles for the reactions of wild-type (black line) and Arg166Ser (red line) AP illustrating the covalent and noncovalent interactions with phosphate. Energy changes are relative to free enzyme and phosphate (E + P_i), and use standard states of 10 mM P_i and 1 nM enzyme. The values used to obtain these profiles are listed in Table 4, and energies were determined as described in Methods.

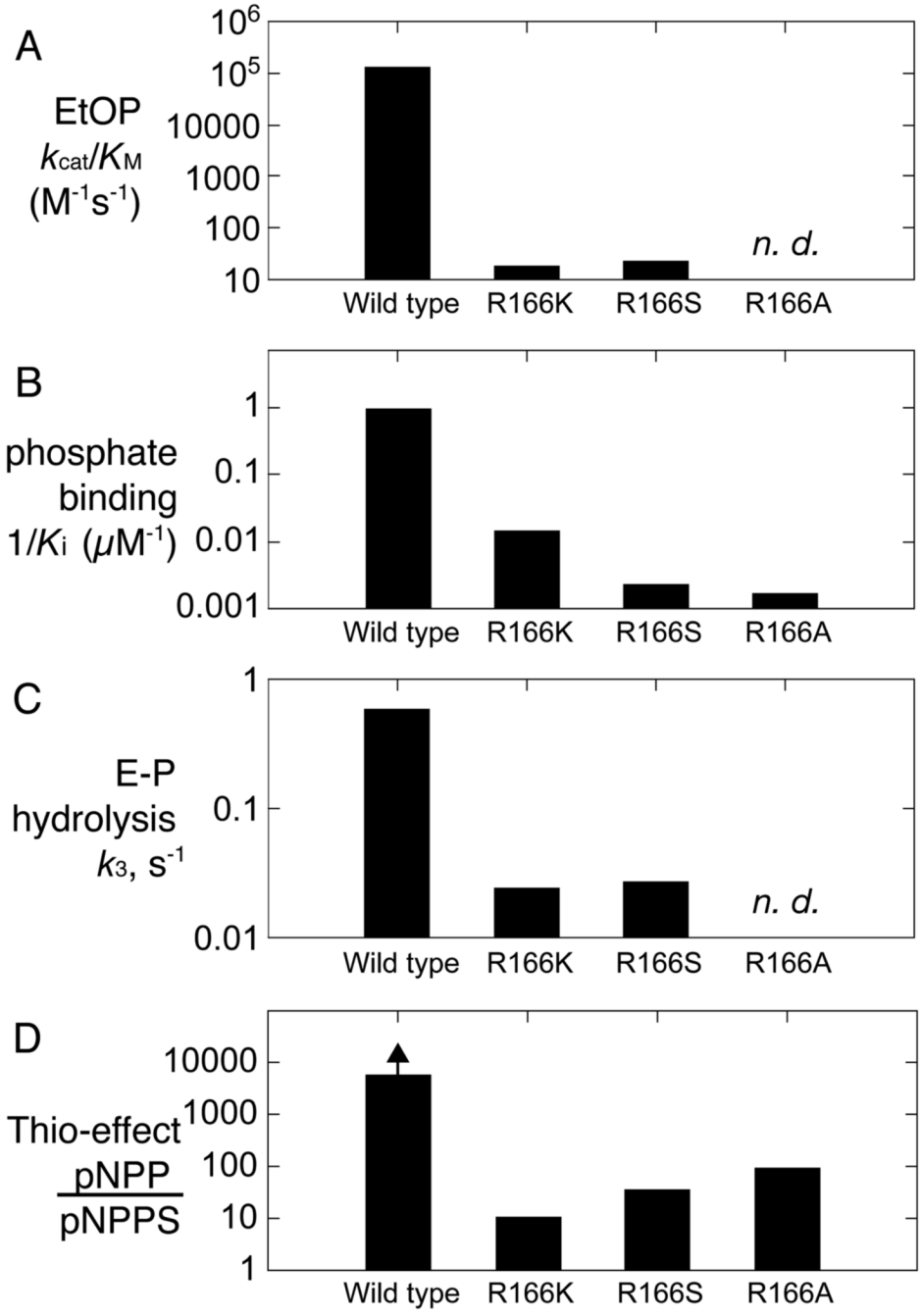

Figure 4.

Effect of mutation of the active site Arg of *E. coli* AP on different reactions and reaction steps. All data are plotted on log scales. (A) Effect on overall reaction with ethyl phosphate. The k_{cat}/K_M values are from Table 1. In contrast to activated aryl phosphates, the chemical step for EtOP hydrolysis is rate-limiting for wild-type enzyme, so that the full catalytic consequences (on binding and cleavage of the RO-P bond) of each mutant can be assessed. (B) Effect on binding of P_i. The association constants, $K_a = (1/K_i)$, were calculated from the data in Table 2. (C) Effect on cleavage of the E-P species at 0 °C and pH 7 (k_3, Scheme 1). Values for wild type and Arg166Ser are from Table 4. The value for Arg166Lys is an estimate of 0.021 s^{-1} based on k_{cat}, as evidence suggests that k_{cat} is limited by k_3 for Arg166Lys (see footnote in

main text). (D) Effect on the observed thio-effect with a *p*-nitrophenolate leaving group. Data are from Table 5. Note that the effect for wild type is a lower limit, because reaction with pNPP is diffusion limited.

Table 1

Effect of Arg166 mutation on AP-catalyzed hydrolysis of phosphate esters.

Enzyme	pNPP			EtOP	
	k_{cat} (s^{-1})	k_{cat}/K_M ($M^{-1}s^{-1}$)	Fold reduction[a]	k_{cat}/K_M ($M^{-1}s^{-1}$)	Fold reduction[a]
Wild type	12[b]	3.3×10^{7}[c]	(1)	1.4×10^{5}[c]	(1)
Arg166Lys	0.65[d]	1.9×10^{5}[d]	170	2.0×10^{1}	7000
Arg166Ser	0.5[e]	1.0×10^{5}[e]	330	2.4×10^{1}	5800
Arg166Ala[f]	0.3	2×10^{4}	1700	-	-

Steady-state rate constants are from this work unless otherwise indicated and are reported per active site, assuming two active sites per dimer. Reaction conditions are 0.1 M MOPS pH 8.0, 0.5 M NaCl, 1 mM $MgCl_2$, 100 μM $ZnSO_4$ at 25 °C (see Methods for details).

[a] Fold reduction is obtained by dividing k_{cat}/K_M for the wild-type enzyme with that for the mutant enzyme.

[b] The rate-limiting step for k_{cat} in wild-type AP may be mixed at this ionic strength, pH and temperature (k_3 & k_4, scheme 1), but k_3 is likely limiting for the mutants (see footnote in Results).

[c] Values from (33), measured under identical conditions.

[d] Values are in reasonable agreement with the previously reported k_{cat} value of 2.2 s^{-1} and k_{cat}/K_M of 4.2×10^5 $M^{-1}s^{-1}$ that were measured in 50 mM Tris-HCl, pH 8, at an ionic strength of 200 mM (44).

[e] Values are in reasonable agreement of the previously reported rate constants of k_{cat} = 0.44 s^{-1} and $k_{cat}/K_M = 6 \times 10^4$ $M^{-1}s^{-1}$ that were measured under similar reaction conditions (43).

[f] Two previous studies (32,43) have reported steady state kinetic parameters for the Arg166Ala mutant of k_{cat} = 0.33 s^{-1} and 0.29 s^{-1}; k_{cat}/K_M = 2.4×10^4 and 1.7×10^4 M^{-1} s^{-1}, and the average values are included here for comparison to the other Arg166 variants. The activity of this mutant with EtOP has not been reported.

Table 2

Effect of Arg166 mutations on binding of inorganic phosphate by alkaline phosphatase.

Enzyme	K_i (μM) [a]	Relative K_i
Wild type	1.1 ± 0.2 [b]	(1)
Arg166Lys	75 ± 10	68
Arg166Ser	460 ± 40 [c]	420
Arg166Ala	650 [d]	590

[a] The inhibition constant for Arg166Lys was measured with pNPP as a substrate under the standard reaction conditions (see Methods). We compare the newly measured inhibition of the Arg166Lys mutant to previously published results for other Arg166 variants.

[b] From (33).

[c] From (45); a similar value of 417 μM has been reported for this mutant (43).

[d] Two previous studies reported K_i values of 643 (43) and 665 μM (32) for this mutant, and the average value is reported.

Table 3

X-ray crystallographic data collection and refinement statistics

	Arg166Ser AP
Space Group	$P6_322$
Unit Cell	
a	160.6 Å
b	160.6 Å
c	139.9 Å
Wavelength	0.9795 Å
Resolution range	38.8 Å–2.1 Å
I/σ [a]	21.3 (2.2)
Total reflections	8,145,677
Unique reflections	63,497
Completeness[a]	99.9% (99.8%)
Redundancy[a]	26.7 (18.7)
R_{merge} [a,b]	0.18 (0.93)
R_{factor}	0.18
R_{free}	0.21
Estimated coordinate error[c]	0.11 Å
Number of residues	890
Number of water molecules	271
Mean B value	28.0 $Å^2$
RMSD from standard geometry	
bond lengths	0.017 Å
bond angles	1.6°
Ramachandran plot statistics	
Most favored regions	91.1%
Additional allowed regions	8.9%
Others	0%

[a] Values in parentheses are for the highest resolution shell.

[b] $R_{merge} = \Sigma| I_{obs} - I_{ave}| / \Sigma I_{obs}$; values are large due to high redundancy.

[c] Based on maximum likelihood estimation.

Table 4

Rate and equilibrium constants for hydrolysis and formation of the covalent E-P complex for wild-type and Arg166Ser alkaline phosphatase at 0 °C.

Kinetic Parameter	Wild-type	Arg166Ser
K_3	99 ± 17	38 ± 4
k_3 (s^{-1})	0.6 ± 0.1	0.028 ± 0.004
k_{-3} (s^{-1})	0.006	0.0007
K_4 (M)	$1.1 \pm 0.1 \times 10^{-6}$	$4.6 \pm 0.2 \times 10^{-4}$
k_4 (s^{-1})	36	1.5×10^4
k_{-4} ($M^{-1}s^{-1}$)	3.3×10^7	3.3×10^7

Rate and equilibrium constants are defined in Scheme 1. As rate constants were too fast to measure by hand under the standard reaction conditions, we analyzed the rate and equilibrium constants at lower pH and lower temperature. The kinetic and thermodynamic data shown were collected in 0.1 M MOPS, pH 7.0, 0.5 M NaCl, 1 mM $MgCl_2$, 0.1 mM $ZnSO_4$ at 0 °C. The equilibrium constant K_3 (= k_3/k_{-3}) is the observed equilibrium of [E•P]/[E-P]. This value assumes that the AP dimer can form two covalent intermediates (one P_i per active site). It is not known if alkaline phosphatase exhibits half-sites reactivity, but if it does, calculated values of K_3 would be overestimated by two-fold. However, neither the values of k_3 nor any of the comparisons of wild-type and R166S AP would be affected. The rate constant for hydrolysis of the covalent intermediate, k_3, was directly observed by measuring breakdown of a radioactive E-P complex (see Materials and Methods). This rate constant was the same as k_{cat} measured for both wild type and Arg166Ser at a several pH values and temperatures (data not shown). The rate constant for phosphorylation of the enzyme, k_{-3}, was calculated from the measured values of k_3 and K_3 ($k_{-3} = k_3/K_3$). The equilibrium constant K_4 is accurately described by the inhibition constant for phosphate, because at alkaline pH negligible covalent complex is formed. The rate constant for phosphate binding, k_{-4}, was not directly measured; we used the k_{cat}/K_M value for fast substrates, which apparently are limited by binding (22,62,63), as an estimate for the rate of P_i binding. For the wild-type enzyme, this assumption yields a value of k_4 that is in good agreement with k_4 measured by ^{31}P NMR inversion transfer experiments (55). We assumed that the Arg166Ser mutation does not affect the rate constant for binding. The rate constant for phosphate release, k_4, was calculated from the equilibrium constant and the assumed binding rate constant ($k_4 = k_{-4}K_4$).

Table 5

Thio effects for reactions of wild type and mutant alkaline phosphatase.

Enzyme	k_{cat}/K_M ($M^{-1}s^{-1}$)		Thio effect
	pNPP	pNPPS	
Wild-type	3.3×10^7	5.5×10^3	6000 [a]
Arg166Lys	1.9×10^5	1.6×10^4	12
Arg166Ser	1.0×10^5	2.6×10^3	38
Arg166Ala [b]	2×10^4	2×10^2	100
No enzyme [c]	2.5×10^{-11}	1.9×10^{-10}	0.13

The k_{cat}/K_M values for pNPP hydrolysis are from Table 1, and the values for pNPPS are from the current study unless otherwise indicated (See Methods for experimental details). Reaction conditions are 0.1 M MOPS pH 8.0, 0.5 M NaCl, 1 mM $MgCl_2$, 100 μM $ZnSO_4$ at 25 °C. The thio-effect is defined here as the ratio of k_{cat}/K_M for the normal substrate, pNPP, divided by that of the sulfur-substituted analog, pNPPS.

[a] The observed thio-effect for the wild-type enzyme is a lower limit for the true impact of sulfur substitution in the transition state for the reaction, because k_{cat}/K_M for pNPP is limited by a non-chemical step (22,62,63).

[b] From ref 32.

[c] Values for nonenzymatic hydrolysis of pNPP and pNPPS are from (20) and (68), respectively. Values were converted into a second order rate constant by dividing by the concentration of the nucleophile (water = 55.5 M).